ChemPubSoc Europe
DOI: 10.1002/chem.201406271
CHEMISTRY
A European Journal
Full Paper

Reaction Mechanisms

Experimental and Computational Insights into Carbon Dioxide Fixation by RZnOH Species

Kamil Sokołowski,[a] Wojciech Bury,[b] Adam Tulewicz,[b, c] Anna M. Cieślak,[a] Iwona Justyniak,[a] Dominik Kubicki,[b] Elżbieta Krajewska,[b] Anne Milet,[d] Robert Moszyński,[c] and Janusz Lewiński*[a, b]

Dedicated to Professor Herbert W. Roesky on the occasion of his 80th birthday

Abstract: Organozinc hydroxides, RZnOH, possessing the proton-reactive alkylzinc group and the CO_2-reactive Zn–OH group, represent an intriguing group of organometallic precursors for the synthesis of novel zinc carbonates. Comprehensive experimental and computational investigations on 1) solution and solid-state behavior of *t*BuZnOH (**1**) species in the presence of Lewis bases, namely, THF and 4-methylpyridine; 2) step-by-step sequence of the reaction between ***1*** and CO_2; and 3) the effect of a donor ligand and/or an excess of tBu_2Zn as an external proton acceptor on the reaction course are reported. DFT calculations for the insertion of carbon dioxide into the dinuclear alkylzinc hydroxide $\mathbf{1}_2$ are fully consistent with ^1H NMR spectroscopy studies and indicate that this process is a multistep reaction, in which the insertion of CO_2 seems to be the rate-determining step. Moreover, DFT studies show that the mechanism of the rearrangement between key intermediates, that is, the primary alkylzinc bicarbonate with a proximal position of hydrogen and the secondary alkylzinc bicarbonate with a distal position of hydrogen, most likely proceeds through internal rotation of the dinuclear bicarbonate.

Introduction

Over the last decade, fixation approaches for CO_2 sequestration have received much attention because of their great environmental significance and very promising practical applications in materials chemistry.[1] Indeed, in Nature, CO_2 is the most abundant C-1 building block that is widely used to synthesize complex organic molecules in living organisms. In synthetic chemistry, CO_2 can be also utilized as a C-1 chemical feedstock for the preparation of useful carbon-containing organic compounds in metal-catalyzed systems.[1c–g] However, the construction of functional materials based on CO_2–metal carbonate conversion is much less explored and such materials are mostly isolated accidentally.[2] Particularly intriguing examples of CO_2 fixation concern reaction systems patterned on the active center of carbonic anhydrase (CA), which contains the Zn–OH group.[3]

Surprisingly, although a number of zinc complexes supported by multidentate ligands and terminal or bridging hydroxide ligation have been widely investigated experimentally as synthetic analogues of CA,[3,4] related organozinc hydroxide compounds have not been explored in this context.[5] Recently our group demonstrated that RZnOH-type moieties featuring a CO_2-reactive Zn–OH group and a proton-reactive Zn–C bond (Scheme 1 a) possessed the unique ability to fix CO_2 and afforded various zinc carbonate products (Scheme 1 b). These preliminary investigations provided the first example of a structurally characterized alkylzinc hydroxide, *t*BuZnOH (**1**),[6] which, in the presence of CO_2, can form different nanomaterials based on CO_3^{2-} as a templating ion, for example, $ZnCO_3$ nanoparticles (NPs) or discrete alkylzinc carbonate cluster **2** (Scheme 1 b).[7] Moreover, the introduction of an auxiliary ligand, L, to the RZnOH system,[8] followed by the reaction with CO_2, led to the formation of the nanosized cluster $[(L_2Zn)_6(ZnCO_3)_4]$ (L = deprotonated 8-hydroxyquinoline; Scheme 1 b), which self-assembled into noncovalent porous material **WUT-1**.[9] Thus, aside from its fundamental novelty, organozinc hydroxides, in combination with CO_2, have appeared

---

[a] *K. Sokołowski, A. M. Cieślak, Dr. I. Justyniak, Prof. J. Lewiński*
Institute of Physical Chemistry, Polish Academy of Sciences
Kasprzaka 44/52, 01-224 Warsaw (Poland)

[b] *Dr. W. Bury, A. Tulewicz, D. Kubicki, E. Krajewska, Prof. J. Lewiński*
Faculty of Chemistry, Warsaw University of Technology
Noakowskiego 3, 00-664 Warsaw (Poland)
Fax: (+48) 22-3433333
E-mail: lewin@ch.pw.edu.pl
Homepage: http://lewin.ch.pw.edu.pl

[c] *A. Tulewicz, Prof. R. Moszyński*
Department of Chemistry, University of Warsaw
Pasteura 1, 02-093 Warsaw (Poland)

[d] *Prof. A. Milet*
Département de Chimie Moléculaire, équipes CIRE et CT
Université Joseph Fourier UMR-CNRS 5250
ICMG FR-2607, BP 53, 38041 Grenoble Cedex 9 (France)

Supporting information for this article is available on the WWW under http://dx.doi.org/10.1002/chem.201406271.

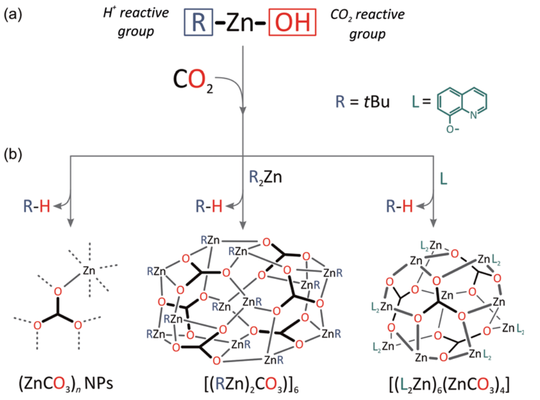

Scheme 1. a) Schematic representation of reactive species in a RZnOH moiety. b) The transformations of the RZnOH/CO_2 reaction systems (from the left) to a mesoporous solid based on $ZnCO_3$ nanoparticles,[7] an organozinc carbonate nanocluster [(*t*BuZn)$_2$(CO$_3$)]$_6$ (**2**),[7] and [(L$_2$Zn)$_6$(ZnCO$_3$)$_4$] as a nanosized molecular building block of the microporous material **WUT-1**.[9]

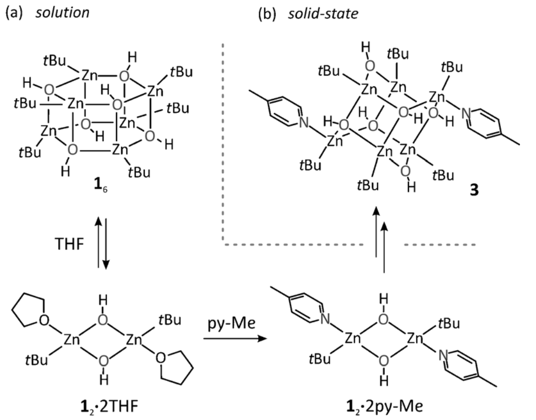

Scheme 2. a) The aggregates of **1** formed in THF, and in the presence of py-Me. b) The transformation of $\mathbf{1_2}$·2 py-Me to **3** upon crystallization from a solution in THF.

as very promising precursors of zinc carbonate based functional materials.

The unprecedented reactivity of the RZnOH/CO_2 system in different coordination environments prompted us to carry out the detailed experimental and computational mechanistic study reported herein. We selected **1** as a model system for CO_2 fixation.[7,9] In particular, we were interested in 1) the solution and solid-state behavior of **1** in the presence of Lewis bases, namely, THF and 4-methylpyridine (py-Me); 2) the sequence of elementary steps of the reaction between **1** and CO_2; and 3) the effect of a Lewis base and an excess of *t*Bu$_2$Zn on the reaction course.

Results and Discussion

Structure of adducts of 1 with Lewis bases

We demonstrated previously that **1** exists in the solid state as a hexameric cluster [*t*BuZn(μ_3-OH)]$_6$ ($\mathbf{1_6}$).[6] To better understand the reaction between **1** and CO_2, first we investigated the character of aggregates that **1** forms in the presence of donor solvents, namely, THF and py-Me. Diffusion-ordered NMR spectroscopy (DOSY) revealed that **1** in [D$_8$]THF[10] exists as a mixture of the hexameric cluster $\mathbf{1_6}$ ($M_{calcd} = 837\ g\,mol^{-1}$; $M_{exptl} = (845 \pm 70)\ g\,mol^{-1}$) and a dimeric species solvated by THF, [*t*BuZn(μ-OH)(THF)]$_2$ ($\mathbf{1_2}$·2 THF; $M_{calcd} = 423\ g\,mol^{-1}$, $M_{exptl} = (436 \pm 44)\ g\,mol^{-1}$; Scheme 2 a, see also Figure S2 and Table S2 in the Supporting Information).[11] The DOSY NMR spectroscopy experiment for an equimolar mixture of **1** and py-Me in [D$_8$]THF revealed that, in this case, only the dimeric alkylzinc hydroxide adduct with py-Me [*t*BuZn(μ-OH)(py-Me)]$_2$ ($\mathbf{1_2}$·2py-Me; $M_{calcd} = 465\ g\,mol^{-1}$, $M_{exptl} = (539 \pm 54)\ g\,mol^{-1}$) was spectroscopically detectable (Scheme 2 a and Figure S4 and Table S3 in the Supporting Information). Recrystallization of an equimolar mixture of **1** and py-Me from a solution in THF at 273 K afforded colorless crystals of a new hexanuclear aggregate stabilized by two py-Me molecules, [*t*Bu$_6$Zn$_6$(μ_3-OH)$_4$(μ-OH)$_2$(py-Me)$_2$] (**3**), as the least soluble product (Scheme 2 b). We note that **3** was also isolated in high yield from a mixture of $\mathbf{1_6}$ with 0.33 equivalents of py-Me (for details, see the Supporting Information). In THF, compound **3** dissociates to form solvated dimeric aggregates of $\mathbf{1_2}$·(py-Me)$_x$(THF)$_{2-x}$ (in which $x = 0$, 1, or 2), as indicated by DOSY NMR spectroscopy experiments (Figure S3 and Table S3 in the Supporting Information). Single-crystal XRD analysis revealed that, in the solid state, compound **3** occurs as a Zn$_6$O$_6$ cage-like structure composed of two Zn$_3$O$_3$ rings in the fused boat conformation (Figure 1). Its molecular structure can be described as being derived from the opening of two opposite edges of the hexagonal prism of $\mathbf{1_6}$. In the Zn$_6$O$_6$ core, two types of hydroxide groups can be distinguished: four of them adopt μ_3-OH and two of them μ-OH coordination modes. The Zn–O bond lengths in Zn–μ_3-O fall within the range of 2.036–2.132 Å and the mean distance of Zn–μ-O is equal to 1.950 Å. In the case of the hexanuclear aggregate **3** stabilized by two py-Me molecules, the described structural features may be attributed to the latent Lewis acidity of the alkylzinc hydroxide cluster, and this behavior resembles the reactions of hexameric *tert*-butylalumoxane with amines.[12]

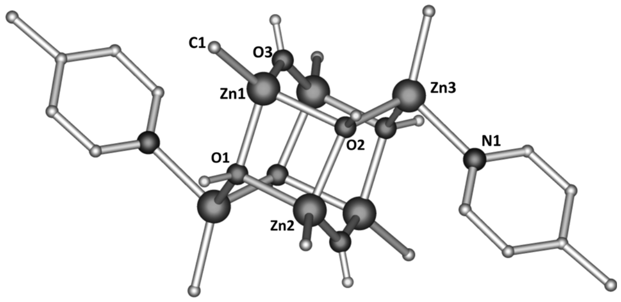

Figure 1. Molecular structure of **3**; methyl groups of the *tert*-butyl groups and hydrogen atoms in py-Me have been omitted for clarity. Selected bond lengths [Å] and angles [°]: Zn1–C1 2.002(8), Zn1–O1 2.082(5), Zn1–O2 2.132(5), Zn1–O3 1.945(5), Zn2–O1 2.055(5), Zn2–O2 2.092(5), Zn3–O2 2.036(5), Zn3–N1 2.145(7); Zn1-O1-Zn2 95.21(19), Zn1-O2-Zn2 92.7(2), Zn1-O2-Zn3 112.0(2), Zn1-O3-Zn2 137.6(1), Zn2-O2-Zn3 130.5(3).

Reactivity of 1 towards CO_2 in the presence of Lewis bases

To investigate the sequence of elementary steps of the reaction between **1** and CO_2 in the presence of Lewis bases, we monitored this reaction by using ^{1}H NMR spectroscopy (Figure 2). Upon exposure of a solution of **1** in [D$_8$]THF to CO_2 at 298 K, we initially observed broadening of the parent Zn–OH signal, which suggested that the zinc-bound hydroxide groups interacted with CO_2 to form incipient complexes (Figure 2 a and Figure S5 in the Supporting Information). After 10 min, new signals at $\delta = 1.16$ and 9.86 ppm emerged; these could be attributed to the bicarbonate species [*t*BuZn(HCO_3)].[13] The resulting highly acidic bicarbonates undergo further transformations by promoting protonolysis of the alkylzinc moieties; this is accompanied by the evolution of isobutane (the corresponding signal appears in the spectrum after ca. 40 min) and the formation of a [$ZnCO_3$] species (Scheme 3).

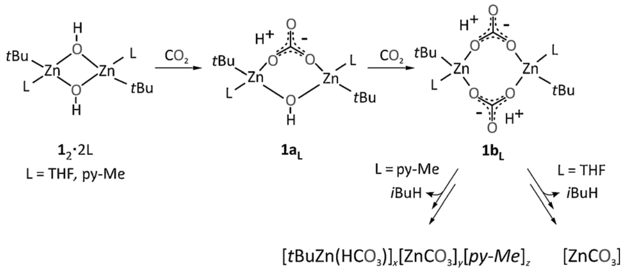

Scheme 3. Proposed sequence of elementary steps in the reaction of $\mathbf{1_2}\cdot 2L$ (L = THF or py-Me) with CO_2.

After 5 h, the only signal that remained in the spectrum was that of isobutane, which indicated that all Zn–OH groups were involved in a stepwise CO_2 fixation process. A gel-like, insoluble substance containing $ZnCO_3$ NPs was recovered from the NMR tube after the reaction ended.[7]

To test the effect of py-Me as a strong Lewis base on the reaction between RZnOH species and CO_2, we examined the reactivity of the py-Me adduct **3** towards CO_2 in [D$_8$]THF at 298 K. Again, significant broadening of ZnOH signals was observed (Figure 2 b and Figure S6 in the Supporting Information); however, resonances attributed to [*t*BuZn(HCO_3)] emerged shortly (after around 10 min) and simultaneously signals belonging to **1** ($\delta = 1.05$ and 4.49 ppm) decreased.[14] Strikingly, for the **3**/CO_2 system, we essentially did not observe any signals of isobutane during the first 90 min of the reaction. It is reasonable to assume that at this stage of the process it is the formation of putative dinuclear aggregates ($\mathbf{1\,a}_{\text{py-Me}}$) and ($\mathbf{1\,b}_{\text{py-Me}}$) that occurs predominantly (Scheme 3). We noted that in the meantime partial protonolysis of the *t*Bu–Zn group occurred, leading to a complex aggregate that probably contained [*t*BuZn(HCO_3)] and [$ZnCO_3$] moieties, and supported by py-Me molecules. After 24 h, the reaction mixture became cloudy and an insoluble solid formed. Many attempts to obtain single crystals suitable for single-crystal XRD analysis failed and the composition of the resulting product was only qualitatively elucidated as [*t*BuZn(HCO_3)]$_x$[$ZnCO_3$]$_y$[py-Me]$_z$ by elemental analysis (see the Experimental Section), ^{13}C CPMAS NMR spectroscopy [resonances characteristic for carbon atoms from carbonates ($\delta = 168.0$ ppm, broad signal), *t*Bu–Zn group ($\delta = 34.3$ ppm), and *py-Me* ($\delta = 20.6$, 125.27, 149.81 ppm); see Figure S9 in the Supporting Information] and FTIR spectroscopy. IR bands assignable to the carbonate and bicarbonate species were observed at $\tilde{\nu} = 3420$ (ν(OH)), 1684 (ν_{as}(CO)), 1508 (ν_{as}(CO)), 1463 (ν_s(CO)) (the most intense band), 1380 (ν_{as}(CO)), and 1236 cm^{-1} (δ(OCOH)) (see Figure S10 in the Supporting Information).[15]

Based on the above investigations, it is reasonable to conclude that the consumption of ZnOH moieties takes place faster in the **1**/CO_2/py-Me system compared with that in the **1**/CO_2/THF system, with the concomitant formation of relatively stable alkylzinc bicarbonate [*t*BuZn(HCO_3)]$_n$ species (Scheme 3).

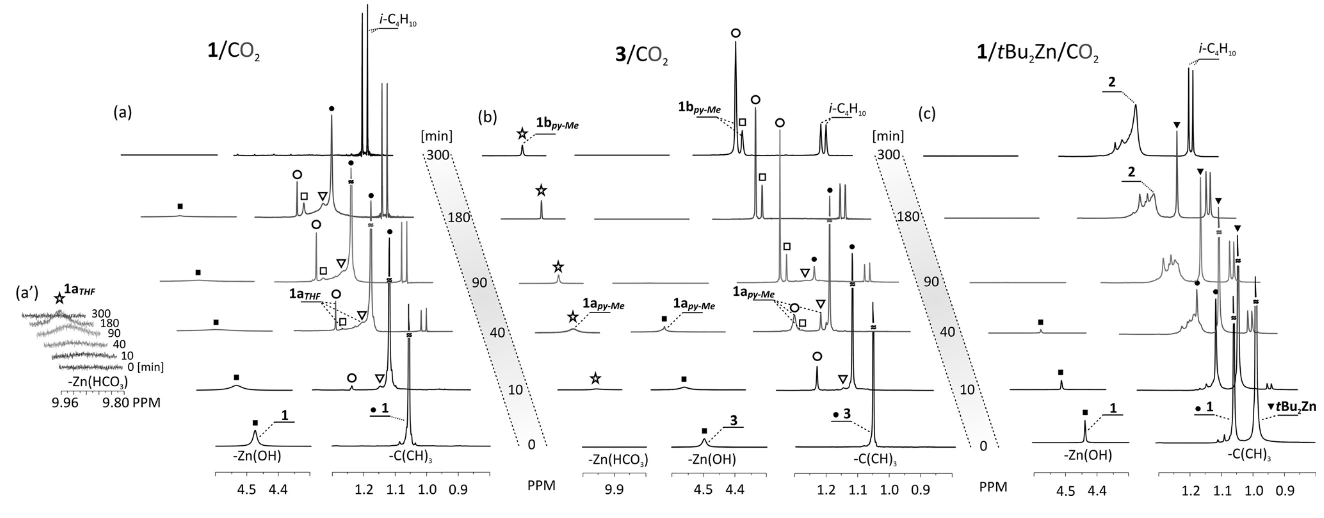

Figure 2. a) ^{1}H NMR spectra for CO_2 fixation by **1** in [D$_8$]THF; a′) inset showing an enlarged spectrum range. b) ^{1}H NMR spectra for CO_2 fixation by **3** in [D$_8$]THF. c) ^{1}H NMR spectra for CO_2 fixation by the **1**/*t*Bu$_2$Zn reaction system in [D$_8$]THF. Characteristic signals are marked as follows: ●, ■: *t*BuZn, Zn(OH) groups from **1** or **3**; ▼: *t*BuZn groups from *t*Bu$_2$Zn; ○, □, ▽: *t*BuZn groups of the putative bicarbonate $\mathbf{1\,a}_L$ and $\mathbf{1\,b}_L$ (L = THF or py-Me); ☆: acidic proton from bicarbonate species.

In this case, the protonolysis of the *t*Bu–Zn group affording zinc carbonates and isobutane is much less pronounced than that in the **1**/CO_2/THF system; this can be attributed to more efficient stabilization of the putative bicarbonate intermediate **1 b**$_L$ by py-Me. Strong donor ligands are liable to significantly modulate the internal rearrangement of the resulting bicarbonate ion and its reactivity; this hypothesis is in agreement with prior theoretical studies of biomimetic systems in which the presence of indirect (external) supporting residues facilitate the proton relay of zinc-bound bicarbonate.[16]

Reactivity of 1 towards CO_2 in the presence of *t*Bu_2Zn

In our previous studies, we demonstrated that the presence of *t*Bu_2Zn had a strong influence on the reaction between **1** and CO_2, yielding the alkylzinc carbonate complex **2**.[7] We hypothesized that in this system excess *t*Bu_2Zn acted as an external proton acceptor and quenched acidic protons in the bicarbonate intermediates **1 a**$_L$ or **1 b**$_L$ (Scheme 3). To investigate the **1**/CO_2/*t*Bu_2Zn system, first we ensured that **1** itself was not reactive towards *t*Bu_2Zn. A control ^{1}H NMR spectroscopy experiment carried out under ambient conditions for an equimolar mixture of **1** and *t*Bu_2Zn in THF and toluene showed that the characteristic signals of both compounds were present and their intensities were unaltered (see the Supporting Information for details). In the next step, we monitored the reaction of **1** with CO_2 in the presence of *t*Bu_2Zn in [D$_8$]THF by using ^{1}H NMR spectroscopy. Figure 2 c reveals that signals attributed to **1** ($\delta = 1.05$ and 4.44 ppm) and *t*Bu_2Zn ($\delta = 0.98$ ppm) disappeared quickly (see also Figure S6 in the Supporting Information), and isobutane was formed during the first 10 min of the reaction. The signals of *t*BuZn gradually disappeared within a few hours, and during the reaction course we did not observe signals characteristic for bicarbonate species (see above). This indicates that the fast transformation of the bicarbonate species into alkylzinc carbonate **2** is triggered by protonolysis of *t*Bu_2Zn molecules. Similar results were obtained in the case of **3**/6*t*Bu_2Zn in [D$_8$]THF exposed to CO_2. As for the **1**/CO_2/*t*Bu_2Zn system, we did not observe any presence of bicarbonate species (Figure S8 in the Supporting Information). Notably, the reaction of **3**/6*t*Bu_2Zn with CO_2 yielded alkylzinc carbonate **2** in high yield (75 %).[17]

DFT calculations

DFT calculations were performed at the PBE0/6-31G++(2d,2p) level[18] to determine the pathway of CO_2 insertion into the dimeric unit [*t*BuZn(μ-OH)]$_2$ (**1**$_2$). We focused on the energy profiles of various elementary steps of the reaction between **1**$_2$ and CO_2, as well as on the mechanism associated with intramolecular rearrangements of the dinuclear [*t*BuZn(μ-OH)][*t*BuZn(HCO_3)] bicarbonate intermediate (Figure 3). We note that theoretical studies considering the mechanism of CO_2 fixation mediated by dinuclear systems are relatively scarce,[19] in contrast to many computational studies on mononuclear CA model systems over the last three decades.[16,20]

The reaction path for the fixation of one molecule of CO_2 into the dimeric **1**$_2$ unit is presented in Figure 3. In the first stage of the reaction, the separated reactants form an encounter complex (a local minimum on the energy pathway) **1**$_2$·CO_2 (**a1**), although the binding energy of -4.9 kJ mol^{-1} does not indicate a strong interaction between the subunits. The closest contact between the hydroxyl oxygen and the CO_2 carbon atom (2.93 Å) for **a1** is shorter than the van der Waals separation estimated from the van der Waals radii (3.22 Å).[21] The next step, in which the bicarbonate TS **a2** is formed, seems to be the most limiting due to the relatively high energetic barrier of $+52.5$ kJ mol^{-1}. At this point, the deviation from linearity of the CO_2 molecule is 32.1°. This barrier exceeds approximately twice that calculated for mononuclear CA model systems.[16b] The reaction is then expected to proceed to the primary bicarbonate [*t*BuZn(μ-OH)][*t*BuZn(HCO_3)] (**a3**) as a local minimum (corresponding to the primary bicarbonate **1 a**$_L$′ in Scheme 4[22]) with a six-membered heterocyclic ring and a bicarbonate proton in the proximal position.

In the case of the CA model systems, at the stage of CO_2 fixation, an intramolecular proton transfer (Lipscomb mechanism) or an internal rotation (Lindskog mechanism) of the bicarbonate species are usually considered.[3c,16,20] In the present case, the activation energy corresponding to direct proton transfer between primary bicarbonate **a3** and secondary bicarbonate **a7** has a value of $+82.7$ kJ mol^{-1} (see Figure S11 in the Supporting Information). The appearance of such a big energy gap in the absence of proton acceptors[23] strongly suggests that the rotation-type mechanism should be expected. During the formation of the bicarbonate group, internal proton transfer to the ternary carbon atom in the *t*Bu group may also occur. This

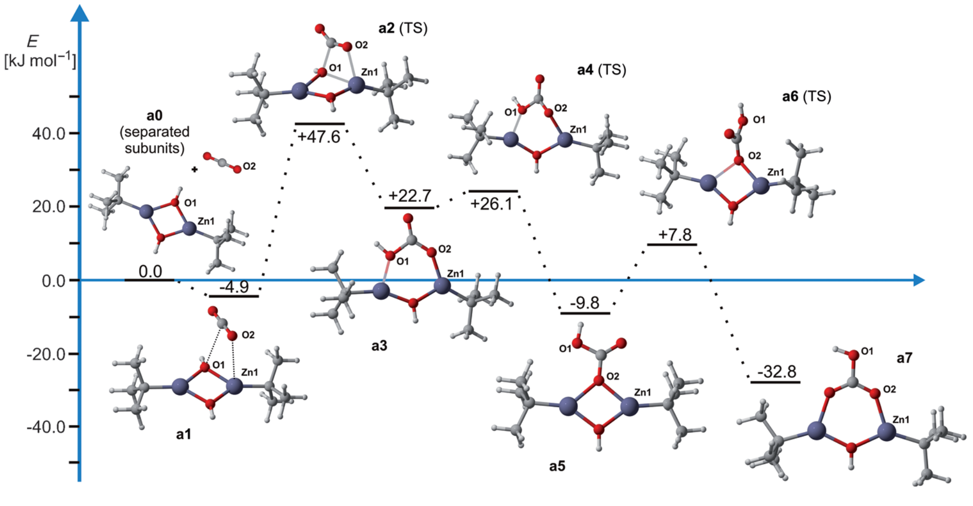

Figure 3. Reaction profile with energetic minima and transition states (TSs) for CO_2 fixation by **1**$_2$. Energy values [kJ mol^{-1}] were obtained at the PBE0/6-31G++(2d,2p) level of theory.

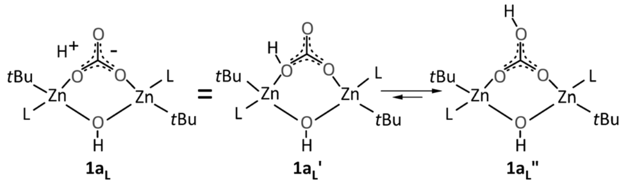

Scheme 4. The proposed equilibrium between primary **1 a**$_L'$ and secondary **1 a**$_L''$ bicarbonate intermediates in a donor solvent (L = THF or py-Me).

competitive process, however, was found to be endothermic (see Figure S12 in the Supporting Information) and had an extremely high activation barrier of $+167.4$ kJ mol^{-1}. Indeed, the energy profile presented in Figure 3 clearly indicates that for the dinuclear [*t*BuZn(μ-OH)][*t*BuZn(HCO$_3$)] intermediate the rotation-type pathway is favored for the transformation from primary bicarbonate **a3** to secondary bicarbonate **a7** and proceeds via local minimum **a5** and two TSs, **a4** and **a6**. The Zn1–O2 bond in structure **a3** first undergoes a transformation to the **a5** local minimum with a four-membered Zn$_2$O$_2$ ring. This transformation proceeds via TS **a4**, and represents an almost negligible energy barrier of 3.4 kJ mol^{-1}. After rotation around the carbon–oxygen bond, separated by TS **a6**, the final product **a7** is obtained (denoted as **1 a**$_L''$ in Scheme 4). The rotation-type pathway of the dinuclear [*t*BuZn(μ-OH)][*t*BuZn(HCO$_3$)] intermediate rearrangement shows considerable similarity to that commonly encountered in bicarbonate intermediates of mononuclear CA model systems. Notably, the CO$_2$ fixation process can occur on two sides of **1**$_2$ (both Zn–OH groups can be involved in the CO$_2$ fixation), leading to the formation of dinuclear [*t*BuZn(μ-OH)][*t*BuZn(HCO$_3$)] and [*t*BuZn(HCO$_3$)]$_2$ bicarbonates. DFT calculations indicate that for both insertion steps the activation energies have comparable values (see Figure S13 in the Supporting Information), which is consistent with our experimental observations (see above).

Moreover, the DFT data indicate that, in the **1**/CO$_2$ systems, bicarbonate intermediates **1 a**$_L$ and **1 b**$_L$ are likely to exist as an equilibrated mixture of the primary bicarbonate **1 a**$_L'$ (or **1 b**$_L'$; with proximal position of hydrogen) and the secondary bicarbonate **1 a**$_L''$ (or **1 b**$_L''$; with distal position of hydrogen). It is reasonable to propose that **1 a**$_L$**"** and **1 b**$_L$**"** are energetically favored, as represented in Scheme 4. In the next step, we considered the proton-transfer process in a reaction between the dimeric bicarbonate [*t*BuZn(HCO$_3$)]$_2$ and *t*Bu$_2$Zn. The corresponding path is presented in Figure 4, and the diagram shows that the reaction starts with the formation of [*t*BuZn(HCO$_3$)]$_2$·*t*Bu$_2$Zn (**b1**), which involves the secondary bicarbonate conformer with the distal position of hydrogen.[24]

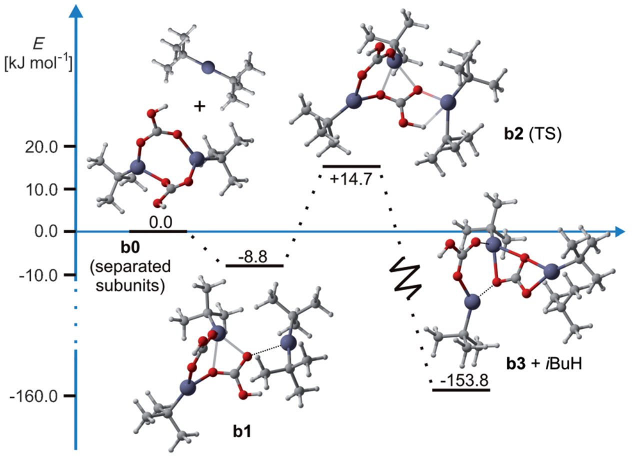

Figure 4. Reaction profile with energetic minima and TSs for the [*t*BuZn(HCO$_3$)]$_2$/*t*Bu$_2$Zn reaction system. Energy values [kJ mol^{-1}] were obtained at the PBE0/6-31G++(2d,2p) level of theory.

As expected, the corresponding binding energy is negative, -8.8 kJ mol^{-1}, mainly due to electrostatic interactions between the oxygen atom on the bicarbonate subunits and the zinc atom from the acceptor molecule. The crucial step of the presented path is then the formation of TS **b2**, which corresponds to the reaction barrier of $+14.7$ kJ mol^{-1}. The formation of TS **b2** enables protonolysis of the Zn–C bond in the external molecule with the formation of a mixed carbonate product [*t*BuZn$_2$(HCO$_3$)(CO$_3$)] (**b3**) and isobutane. Finally, the overall energy gain of the reaction yields a total value of -153.8 kJ mol^{-1}, which is likely to render it essentially irreversible. In conclusion, the DFT calculations, in conjunction with spectroscopic studies, clearly indicate that the presence of *t*Bu$_2$Zn in the **1**/CO$_2$ system greatly accelerates proton transfer from the intermediate bicarbonate species **1 b**$_{THF}''$ and supports the formation of the alkylzinc carbonate [(*t*BuZn)$_2$(CO$_3$)]$_6$[THF]$_2$, as shown in Scheme 5.[22]

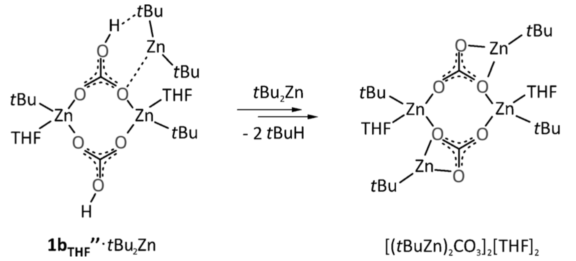

Scheme 5. Proposed transformation of the intermediate bicarbonate **1 b**$_{THF}''$ in the presence of *t*Bu$_2$Zn.

Conclusion

We provided a comprehensive experimental and theoretical study that afforded a detailed mechanistic picture of the reaction between RZnOH species and CO$_2$. We demonstrated that species of **1** in the presence of donor ligand L readily formed dimeric species [*t*BuZn(μ-OH)(L)]$_2$ (L = THF, py-Me) in solution. The ^{1}H NMR spectroscopy studies supported by DFT calculations indicated that in the reaction of **1**$_2$·2 L with CO$_2$ both Zn–OH groups were involved in the fixation of CO$_2$ to form putative primary and secondary dinuclear bicarbonate intermediates. The resulting acidic bicarbonates underwent further transformations by promoting protonolysis of the alkylzinc moieties, which was accompanied by the evolution of isobutane and the formation of [ZnCO$_3$] species. In the case of the **1**/CO$_2$/py-Me system, protonolysis of *t*Bu–Zn group was much less pronounced than that in the **1**/CO$_2$/THF system. Further-more, our studies indicated that the presence of $t\mathrm{Bu_2Zn}$ in the **1**/$\mathrm{CO_2}$ system greatly accelerated proton transfer from the intermediate bicarbonate species and supported the formation of alkylzinc carbonate cluster **2**. In both systems, **1**/$\mathrm{CO_2}$ and **1**/$\mathrm{CO_2}$/$t\mathrm{Bu_2Zn}$, proton transfer from the bicarbonate to the alkylzinc species or external $t\mathrm{Bu_2Zn}$ molecule, respectively, was irreversible and became the driving force for the formation of the final carbonate products. Finally, our studies underlined the increasing potential of simple organozinc precursors that featured $\mathrm{CO_2}$-reactive Zn–OH groups and proton-reactive Zn–C bonds for the design of new functional materials based on zinc carbonate components.

Experimental Section

Methods and materials

All manipulations were conducted under a nitrogen atmosphere by using standard Schlenk techniques. Di-*tert*-butylzinc[25] and **1**[7] were prepared as described previously. All other reagents were purchased from commercial vendors (py-Me (Aldrich), $\mathrm{CO_2}$ 99.999 % (Multax)), and solvents were dried and distilled from Na/K alloy prior to use. Solution NMR spectra were acquired on Varian Mercury 400 MHz and Varian Inova 500 MHz spectrometers. Solid-state NMR spectra were acquired on a Bruker Avance II 500 MHz spectrometer. IR spectra were recorded on an FTIR PerkinElmer System 2000 spectrometer.

Synthesis of 3

Lewis base py-Me (16 μL, 0.16 mmol, 0.33 equiv) was added to a freshly prepared solution (12.0 mL) of $\mathbf{1}_6$ (0.420 g, 0.50 mmol) in THF. The prepared solution was stirred at room temperature for 1 h. Compound **3** was obtained as colorless plate-like crystals after recrystallization from THF at −20 °C (0.412 g, 81 %). ^{1}H NMR ([$\mathrm{D_8}$]THF, 400.10 MHz, 298 K): $\delta=7.11$ (d, 2H; $\mathrm{CH_{Pr}}$), 8.38 (d, 2H; $\mathrm{CH_{Pr}}$), 4.49 (s, 1H; ZnOH), 2.32 (s, 3H; $\mathrm{CH_3}$), 1.05 ppm (s, 9H; $\mathrm{ZnC(CH_3)_3}$); IR (Nujol): $\tilde{\nu}=3648$ (s), 3607 (s), 2954 (s), 2924 (s), 2854 (s), 2805 (s), 2746 (w), 2688 (w), 1622 (s), 1461 (s), 1377 (s), 1070 (w), 1023 (m), 914 (s), 803 (s), 722 (m), 656 $\mathrm{cm^{-1}}$ (s); elemental analysis calcd (%) for $\mathrm{C_{36}H_{74}N_2O_6Zn_6}$ (1023.31 $\mathrm{g\,mol^{-1}}$): C 42.23, H 7.23, N 2.74; found: C 42.32, H 7.29, N 2.70;

Reaction of the 3/6 $t\mathrm{Bu_2Zn}$ system with $\mathrm{CO_2}$

A solution of $t\mathrm{Bu_2Zn}$ (0.270 g, 1.50 mmol) in THF (3.0 mL) was added to a freshly prepared solution of **3** (0.256 g, 0.25 mmol) in THF (4.0 mL). The resultant solution was allowed to warm to room temperature and exposed to a $\mathrm{CO_2}$ atmosphere in a Schlenk flask without stirring. Colorless rhomboid crystals of **2** were obtained after recrystallization from the parent mixture at room temperature after 24 h (0.392 g, 88 %).

Reaction of 3 with $\mathrm{CO_2}$

Freshly dissolved **3** (0.268 g, 0.25 mmol) in toluene (4.0 mL) was exposed to a $\mathrm{CO_2}$ atmosphere in a Schlenk flask without stirring. A white, insoluble in organic solvent precipitate was obtained after 24 h. ^{1}H NMR ([$\mathrm{D_8}$]THF, 400.10 MHz, 298 K): $\delta=7.18$ (d, 2H; $\mathrm{CH_{Py}}$), 7.12 (d, 2H; $\mathrm{CH_{Py}}$), 2.30 (s, 3H; $\mathrm{CH_3}$), 1.05 ppm (s, 9H; $\mathrm{ZnC(CH_3)_3}$); CP-MAS ^{13}C NMR: $\delta=20.6$ (4-*py*-$\mathrm{CH_3}$), 34.3 ($C\mathrm{(CH_3)_3}$), 125.3, 149.8 (4-*py*-Me), 168.0 ($\mathrm{CO_3^{2-}}$) ppm; IR (Nujol): $\tilde{\nu}=3383$ (w), 2954 (s), 2923 (s), 2853 (s), 1623 (s), 1505 (w), 1463 (s), 1456 (s), 1377 (s), 1232 (s), 1212 (m), 1069 (m), 1033 (s), 842 (s), 814 (s), 722 $\mathrm{cm^{-1}}$ (m); elemental analysis calcd (%) for $[t\mathrm{Bu_6Zn_6(HCO_3)_6}(Me\text{-}Py)_6]$ $\mathrm{C_{42}H_{74}N_2O_{18}Zn_6}$ (1285.31 $\mathrm{g\,mol^{-1}}$): C 39.22, H 5.76, N 2.17, Zn 30.58; found: C 25.58, H 2.61, N 2.71, Zn 45.48.

Elemental analysis indicated 1) that the molar ratio of py-Me/Zn was 1:3.5 in the precipitate, which corresponded to the composition of starting compound **3** (py-Me/Zn molar ratio 1:3); and 2) the lower content of carbon (in comparison with $[t\mathrm{Bu_6Zn_6(HCO_3)_6(Me\text{-}Py)_6}]$) suggested partial hydrolysis of *t*Bu groups and the formation of carbonate species.

Crystallographic data

Data were collected by using the oil drop technique to mount crystals on a Nonius Kappa-CCD equipped with an Oxford Cryostream low-temperature device.

Crystal data for 3: $\mathrm{C_{36}H_{74}N_2O_6Zn_6}$; $M_r=1023.31$; crystal dimensions $0.34\times0.28\times0.24$ $\mathrm{mm^3}$; triclinic; space group $P\bar{1}$ (no. 2); $a=10.5370(4)$, $b=14.4060(6)$, $c=15.7430(5)$ Å; $\alpha=90.830(2)$, $\beta=99.481(2)$, $\gamma=96.747(2)^\circ$; $U=2339.36(15)$ Å^3; $Z=2$; $F(000)=1064$; $\rho_{\mathrm{calcd}}=1.453$ $\mathrm{g\,m^3}$; $T=100(2)$ K; $\mu(\mathrm{Mo_{K\alpha}})=3.065$ $\mathrm{mm^{-1}}$; $\theta_{\max}=24.71^\circ$; 7957 unique reflections. The structure was solved by direct methods by using the SHELXS97[26] program and was refined by full-matrix least squares on F^2 by using the program SHELXL97.[27] All non-hydrogen atoms were refined with anisotropic displacement parameters. The hydrogen atoms were introduced at geometrically idealized coordinates with a fixed isotropic displacement parameter equal to 1.2. Refinement converged at $R1=0.0751$, $wR2=0.1595$ for all data and 471 parameters ($R1=0.0576$, $wR2=0.1371$ for 6155 reflections with $I_o>2\sigma(I_o)$). The GooF on F^2 was 1.023. A weighting scheme $w=[\sigma^2(F_o^2+(0.0418P)^2+3.1964P]^{-1}$, in which $P=(F_o^2+2F_c^2)/3$ was used in the final stage of the refinement. The residual electron density is $+0.85/-0.75$ $\mathrm{e\,\text{Å}^{-3}}$.

CCDC-866666 contains the supplementary crystallographic data for this paper. These data can be obtained free of charge from The Cambridge Crystallographic Data Centre via www.ccdc.cam.ac.uk/data_request/cif.

Computational details

The geometries of the compounds studied herein were optimized with the PBE0[28] functional in the 6-31G++(2p,2d) basis set (double zeta with the addition of polarized and diffuse functions). The selection of the functional was based on its reliable performance in related calculations when considering mostly higher-row transition-metal complexes,[29,30] and the results were usually comparable or better to those obtained with the popular B3LYP functional for minima and TSs.[31,32] However, contrary to B3LYP, PBE0 represents a parameter-free DFT model.[28]

The nature of the minima and maxima obtained after the optimization process was confirmed by frequency analysis, and zero-point energy corrections were added to the corresponding electronic energies corrected for the basis set superposition error. Additionally, the intrinsic reaction coordinate calculations and the analysis of frequencies were performed for the TSs to check whether the corresponding minima had been correctly located. All calculations were performed with the Gaussian suite of codes.[33] Figures were prepared with the CYLview visualization software.[34]

Acknowledgements

We would like to acknowledge the European Union, Regional Development Fund within a project of Foundation for Polish Science (TEAM/2011-7/8; J.L., I.J., D.K; MPD/2010/4; A.T., J.L., R.M.), the Human Capital Programme (CAS/27/POKL; A.T.), and the Ministry of Science and Higher Education within the Iuventus Plus Programme (IP/2015 015670; K.S.) for financial support. R.M. thanks the Foundation for Polish Science for support within the MISTRZ program in physical sciences. The ICM University of Warsaw Computer Center is acknowledged for facilities and computer time allocation within the grant G44-29.

Keywords: carbon dioxide fixation · computational chemistry · density functional calculations · reaction mechanisms · zinc · zinc hydroxide

[1] a) *Carbon Dioxide as Chemical Feedstock* (Ed.: M. Aresta), Wiley-VCH, Weinheim, **2010**; b) G. A. Olah, G. K. S. Prakash, A. Goeppert, *J. Am. Chem. Soc.* **2011**, *133*, 12881 – 12898; c) M. Cokoja, C. Bruckmeier, B. Rieger, W. A. Herrmann, F. E. Kühn, *Angew. Chem. Int. Ed.* **2011**, *50*, 8510 – 8537; *Angew. Chem.* **2011**, *123*, 8662 – 8690; d) M. Mikkelsen, M. Jørgensen, F. C. Krebs, *Energy Environ. Sci.* **2010**, *3*, 43 – 81; e) T. Sakakura, J. C. Choi, H. Yasuda, *Chem. Rev.* **2007**, *107*, 2365 – 2387; f) D. J. Darensbourg, *Chem. Rev.* **2007**, *107*, 2388 – 2410; g) G. W. Coates, D. R. Moore, *Angew. Chem. Int. Ed.* **2004**, *43*, 6618 – 6639; *Angew. Chem.* **2004**, *116*, 6784 – 6806; h) M. Dupuis, J. G. Ferry, E. Fujita, R. Hille, P. J. A. Kenis, C. A. Kerfeld, R. H. Morris, C. H. F. Peden, A. R. Portis, S. W. Ragsdale, T. B. Rauchfuss, J. N. H. Reek, L. C. Seefeldt, R. K. Thauer, G. L. Waldrop, *Chem. Rev.* **2013**, *113*, 6621 – 6658.

[2] a) S. I. Swamy, J. Bacsa, J. T. A. Jones, K. C. Stylianou, A. Steiner, L. K. K. Ritchie, T. Hasell, J. A. Gould, A. Laybourn, Y. Z. Khimyak, D. J. Adams, M. J. Rosseinsky, A. I. Cooper, *J. Am. Chem. Soc.* **2010**, *132*, 12773 – 12775; b) S.-D. Bian, J.-H. Jia, Q.-M. Wang, *J. Am. Chem. Soc.* **2009**, *131*, 3422 – 3423; c) D. Sun, G.-G. Luo, N. Zhang, R.-B. Huang, L.-S. Zheng, *Chem. Commun.* **2011**, *47*, 1461 – 1463; d) B. Zhang, X. Zheng, H. Su, Y. Zhu, C. Du, M. Song, *Dalton Trans.* **2013**, *42*, 8571 – 8574; e) R. McLellan, J. Rezé, S. M. Taylor, R. D. McIntosh, E. K. Brechin, S. J. Dalgarno, *Chem. Commun.* **2014**, *50*, 2202 – 2204; f) T. N. Hooper, R. Inglis, M. A. Palacios, G. S. Nichol, M. B. Pitak, S. J. Coles, G. Lorusso, M. Evangelisti, E. K. Brechin, *Chem. Commun.* **2014**, *50*, 3498 – 3500.

[3] a) V. M. Krishnamurthy, G. K. Kaufman, A. R. Urbach, I. Gitlin, K. L. Gudiksen, D. B. Weibel, G. M. Whitesides, *Chem. Rev.* **2008**, *108*, 946 – 1051; b) H. Vahrenkamp, *Dalton Trans.* **2007**, 4751 – 4759; c) G. Parkin, *Chem. Rev.* **2004**, *104*, 699 – 767; d) H. Vahrenkamp, *Acc. Chem. Res.* **1999**, *32*, 589 – 596.

[4] For selected examples, see: a) W. Sattler, G. Parkin, *Chem. Sci.* **2012**, *3*, 2015 – 2019; b) D. Huang, O. V. Makhlynets, L. L. Tan, S. C. Lee, E. V. Rybak-Akimova, R. H. Holm, *Proc. Natl. Acad. Sci. USA* **2011**, *108*, 1222 – 1227; c) C. Bergquist, T. Fillebeen, M. M. Morlok, G. Parkin, *J. Am. Chem. Soc.* **2003**, *125*, 6189 – 6199; d) L. Cronin, P. H. Walton, *Chem. Commun.* **2003**, 1572 – 1573; e) C. Bergquist, G. Parkin, *J. Am. Chem. Soc.* **1999**, *121*, 6322 – 6323; f) S. Hikichi, M. Tanaka, Y. Moro-oka, *J. Am. Chem. Soc.* **1993**, *115*, 5496 – 5508; g) A. Looney, R. Han, K. McNeill, G. Parkin, *J. Am. Chem. Soc.* **1993**, *115*, 4690 – 4697; h) E. Kimura, T. Shiota, T. Koike, M. Shiro, M. Kodama, *J. Am. Chem. Soc.* **1990**, *112*, 5805 – 5811.

[5] D. Prochowicz, K. Sokołowski, J. Lewiński, *Coord. Chem. Rev.* **2014**, *270–271*, 112 – 126.

[6] W. Bury, E. Krajewska, M. Dutkiewicz, K. Sokołowski, I. Justyniak, Z. Kaszkur, K. J. Kurzydłowski, T. Płociński, J. Lewiński, *Chem. Commun.* **2011**, *47*, 5467 – 5469.

[7] K. Sokołowski, W. Bury, I. Justyniak, A. M. Cieślak, M. Wolska, K. Sołtys, I. Dzięcielewski, J. Lewiński, *Chem. Commun.* **2013**, *49*, 5271 – 5273.

[8] K. Sokołowski, I. Justyniak, W. Śliwiński, K. Sołtys, A. Tulewicz, A. Kornowicz, R. Moszyński, J. Lipkowski, J. Lewiński, *Chem. Eur. J.* **2012**, *18*, 5637 – 5645.

[9] K. Sokołowski, W. Bury, I. Justyniak, D. Fairen-Jimenez, K. Sołtys, D. Prochowicz, S. Yang, M. Schröder, J. Lewiński, *Angew. Chem. Int. Ed.* **2013**, *52*, 13414 – 13418; *Angew. Chem.* **2013**, *125*, 13656 – 13660.

[10] The room-temperature ^{1}H NMR spectrum of a freshly prepared solution of **1** in [D$_8$]THF features partly overlapping resonances that correspond to different *t*Bu groups. To obtain interpretable data that were well resolved in the diffusion domain, multivariable analysis was used (see the Supporting Information).

[11] This observation is distinct from cryoscopic studies on the EtZnOH system in a donor solvent and related alkylzinc alkoxides (RZnOR); for more details, see: a) W. Kuran, M. Czarnecka, *J. Organomet. Chem.* **1984**, *263*, 1 – 7; b) J. Lewiński, M. Dutkiewicz, M. Lesiuk, W. Śliwiński, K. Zelga, I. Justyniak, J. Lipkowski, *Angew. Chem. Int. Ed.* **2010**, *49*, 8266 – 8269; *Angew. Chem.* **2010**, *122*, 8442 – 8445.

[12] a) Y. Koide, S. G. Bott, A. R. Barron, *Organometallics* **1996**, *15*, 5514 – 5518; the latent acidity is a consequence of the ring strain present in the parent cluster **1**$_6$, for example, see: b) C. J. Harlan, S. G. Bott, A. R. Barron, *J. Am. Chem. Soc.* **1995**, *117*, 6465 – 6474.

[13] Zinc bicarbonate has been an elusive species for spectroscopic characterization for decades, and the bicarbonate ion was only very recently identified in a tris(3-*tert*-butyl-5-methylpyrazolyl)hydroborato zinc complex by low-temperature ^{1}H NMR spectroscopy studies ($\delta = 13.2$ ppm, CD$_2$Cl$_2$, 189 K), see: W. Sattler, G. Parkin, *Polyhedron* **2012**, *32*, 41 – 48; more recently these authors reported the first terminal zinc bicarbonate complexes to be structurally characterized by using XRD; for details, see ref. [4a].

[14] For comparison, in the **1**/CO$_2$ system, we observed a relatively weak intensity of the signal attributed to the acidic proton of the bicarbonate species at $\delta = 9.86$ ppm, which suggested rapid proton migration from *t*BuZn(HCO$_3$) species to a thermodynamically favorable energetic minimum Zn(CO$_3$).

[15] Both the slightly asymmetric character of a broad signal at $\delta = 168.0$ ppm in the ^{13}C CPMAS NMR spectrum (see refs. [4a] and [13a]) and overlapping IR bands in the range characteristic for metal carbonates and bicarbonates of various denticity support the putative product composition; for selected references concerning IR studies of metal carbonates and bicarbonates, see: ref. [4a,g], and a) Z. Sun, L. Jin, S. He, Y. Zhao, M. Wei, D. G. Evans, X. Duan, *Green Chem.* **2012**, *14*, 1909 – 1916; b) H. Noei, C. Wöll, M. Mühler, Y. Wang, *J. Phys. Chem. C* **2011**, *115*, 908 – 914; c) S. T. Korhonen, M. Calatayud, A. O. I. Krause, *J. Phys. Chem. C* **2008**, *112*, 16096 – 16102.

[16] a) A. Bottoni, C. Z. Lanza, G. P. Miscione, D. Spinelli, *J. Am. Chem. Soc.* **2004**, *126*, 1542 – 1550; b) G. P. Miscione, M. Stenta, D. Spinelli, E. Anders, A. Bottoni, *Theor. Chem. Acc.* **2007**, *118*, 193 – 201.

[17] This observation is in agreement with another control experiment in which *t*Bu$_2$Zn is added only 5 h after **3** and CO$_2$ are mixed (when **1 b**·py-Me is observed; according to ^{1}H NMR spectroscopy studies). This gave **2** in almost quantitative yield.

[18] The selection of the functional was based on its good convergence performance with respect to other functionals tested, and its reliability was confirmed within the transition-metal studies.

[19] a) B. Kersting, *Angew. Chem. Int. Ed.* **2001**, *40*, 3987 – 3990; *Angew. Chem.* **2001**, *113*, 4109 – 4112; b) L. Castro, O. P. Lam, S. C. Bart, K. Meyer, L. Maron, *Organometallics* **2010**, *29*, 5504 – 5510; c) M. M. El-Hendawy, N. J. English, D. A. Mooney, *Inorg. Chem.* **2012**, *51*, 5282 – 5288; d) M. M. El-Hendawy, S. Bandaru, N. J. English, D. A. Mooney, *Catal. Sci. Technol.* **2013**, *3*, 2234 – 2243; e) O. J. Cooper, C. Camp, J. Pecaut, C. E. Kefalidis, L. Maron, M. Mazzanti, S. Gambarell, *J. Am. Chem. Soc.* **2014**, *136*, 6716 – 6723.

[20] For selected examples, see: a) J.-Y. Liang, W. N. Lipscomb, *J. Am. Chem. Soc.* **1986**, *108*, 5051 – 5058; b) J.-Y. Liang, W. N. Lipscomb, *Biochemistry* **1987**, *26*, 5293 – 5301; c) D. N. Silverman, S. Linsdkog, *Acc. Chem. Res.* **1988**, *21*, 30 – 36; d) M. Sola, A. Lledos, M. Duran, J. Bertran, *J. Am. Chem. Soc.* **1992**, *114*, 869 – 877; e) K. M. Merz Jr, L. Banci, *J. Am. Chem. Soc.* **1997**, *119*, 863 – 871; f) M. Mauksch, M. Brauer, J. Weston, E. Anders, *ChemBioChem* **2001**, *2*, 190 – 198; g) M. Bräuer, J. L. Perez-Lustres, J. Weston, E. Anders, *Inorg. Chem.* **2002**, *41*, 1454 – 1463; h) S. B. Lesnichin, I. G. Shenderovich, T. Muljati, D. Silverman, H.-H. Limbach, *J. Am. Chem. Soc.* **2011**, *133*, 11331 – 11338.

[21] A. Bondi, *J. Phys. Chem.* **1964**, *68*, 441 – 451.

[22] To simplify DFT calculations, we did not include donor solvent molecules in the initial structures.
[23] M. Hartmann, K. M. Merz, R. van Eldik, T. Clark, *J. Mol. Model.* **1998**, *4*, 355 – 365.
[24] Herein, we only consider the interaction between tBu$_2$Zn and the secondary bicarbonate with the distal position of hydrogen. The interaction involving the primary bicarbonate intermediate with the proximal position of hydrogen exhibits significant steric hindrance that does not allow for the stabilization of any TSs.
[25] J. Lewiński, M. Dranka, W. Bury, W. Śliwiński, I. Justyniak, J. Lipkowski, *J. Am. Chem. Soc.* **2007**, *129*, 3096 – 3098.
[26] G. M. Sheldrick, *Acta Crystallogr. Sect. A* **1990**, *46*, 467 – 473.
[27] G. M. Sheldrick, SHELXS97 and SHELXL97, Programs for Crystal Structure Solution and Refinement, University of Göttingen, Germany, **1997**.
[28] C. Adamo, V. Barone, *J. Chem. Phys.* **1999**, *110*, 6158 – 6170.
[29] M. P. Waller, H. Braun, N. Hojdis, M. Buhl, *J. Chem. Theory Comput.* **2007**, *3*, 2234 – 2242.
[30] M. Bühl, C. Reimann, D. A. Pantazis, T. Bredow, F. Neese, *J. Chem. Theory Comput.* **2008**, *4*, 1449 – 1459.
[31] A. D. Boese, A. M. L. Martin, *J. Chem. Phys.* **2004**, *121*, 3405 – 3416.
[32] Y. Sun, H. Chen, *J. Chem. Theory Comput.* **2014**, *10*, 579 – 588.
[33] Gaussian 09, Revision B.01, M. J. Frisch, G. W. Trucks, H. B. Schlegel, G. E. Scuseria, M. A. Robb, J. R. Cheeseman, G. Scalmani, V. Barone, B. Mennucci, G. A. Petersson, H. Nakatsuji, M. Caricato, X. Li, H. P. Hratchian, A. F. Izmaylov, J. Bloino, G. Zheng, J. L. Sonnenberg, M. Hada, M. Ehara, K. Toyota, R. Fukuda, J. Hasegawa, M. Ishida, T. Nakajima, Y. Honda, O. Kitao, H. Nakai, T. Vreven, J. A. Montgomery, Jr.; J. E. Peralta, F. Ogliaro, M. Bearpark, J. J. Heyd, E. Brothers, K. N. Kudin, V. N. Staroverov, R. Kobayashi, J. Normand, K. Raghavachari, A. Rendell, J. C. Burant, S. S. Iyengar, J. Tomasi, M. Cossi, N. Rega, N. J. Millam, M. Klene, J. E. Knox, J. B. Cross, V. Bakken, C. Adamo, J. Jaramillo, R. Gomperts, R. E. Stratmann, O. Yazyev, A. J. Austin, R. Cammi, C. Pomelli, J. W. Ochterski, R. L. Martin, K. Morokuma, V. G. Zakrzewski, G. A. Voth, P. Salvador, J. J. Dannenberg, S. Dapprich, A. D. Daniels, Ö. Farkas, J. B. Foresman, J. V. Ortiz, J. Cioslowski, D. J. Fox, Gaussian, Inc., Wallingford CT, **2010**.
[34] C. Y. Legault, *CYLview, 1.0b*; Université de Sherbrooke: Sherbrooke, Canada, 2009; http://www.cylview.org.

Received: November 28, 2014